Int. J. Electrochem. Sci., 6 **(2011)** 6456 - 6468

International Journal of
ELECTROCHEMICAL
SCIENCE
www.electrochemsci.org

Fabrication of Multifunctional Biosensor for the Determination of Hydrogen Peroxide, Dopamine and Uric Acid

Tsung-Hsuan Tsai[1], *Yun-Chin Huang*[1], *Shen-Ming Chen*[*, 1] , M. Ajmal Ali[2], Fahad M. A. AlHemaid[2]

[1]Electroanalysis and Bioelectrochemistry Lab, Department of Chemical Engineering and Biotechnology, National Taipei University of Technology, No.1, Section 3, Chung-Hsiao East Road, Taipei 106, Taiwan (ROC).
[*]E-mail: smchen78@ms15.hinet.net

[2]Department of Botany and Microbiology, College of Science, King Saud University, Riyadh- 11451, Saudi Arabia

Received: 10 October 2011 / *Accepted:* 31 October 2011 / *Published:* 1 December 2011

A novel multifunctional biosensor was prepared by dropping graphene on the 2-Amino-thiazol (AT) film at glassy carbon electrode (GCE). The surface morphology of graphene, AT and graphene-AT film modified GCE has been examined by using SEM and AFM. The advantages of proposed film were demonstrated for the determination of H_2O_2 reduction using amperometric, DA and UA oxidation using differential pulse voltammetry. The graphene-AT/GCE as a multifunctional biosensor exhibited a linear response range for H_2O_2 determine (from 1.0×10^{-5} to 3.1×10^{-4} M), low detection limit (10^{-6} M), high sensitivity (1.73 mA mM^{-1} cm^{-2}) and the relative standard deviation (RSD %) less than 2% (n = 5). Similarly, the multifunctional biosensor can simultaneously determine the DA and UA with the interference of AA. For the linear response range of DA and UA were from 5×10^{-6} to 2.5×10^{-5} M and 2.5×10^{-6} to 1.25×10^{-4} M. In addition, the multifunctional biosensor by graphene-AT film modified GCE was advantageous in terms of its simple preparation, specificity, stability and selectivity.

Keywords: Graphene; 2-Amino-thiazol; Multifunctional biosensor; Hydrogen peroxide; Dopamine; Uric acid, Electrochemical, Sensors, modified electrodes.

1. INTRODUCTION

Biosensor has become one of the most important methods in industrial process control, environmental monitoring, and different applications in medicine and biotechnology. The use of bare electrodes in such analysis has numerous limitations such as high overpotential, slow electron transfer

reaction, low sensitivity, lack of reproducibility, poor stability and selectivity [1 - 6]. Fabricate a good biosensor represent the development and exploitation of analytical devices for detection, quantification and monitoring of specific chemical species for clinical, environmental and industrial analysis [7]. In recent years, it would be interesting to perform a multifunction biosensor, such as the determination of H_2O_2 and glucose by histidine/nickel hexacyanoferrate nanotube film [8], carbon nanotube/chitosan/gold nanoparticles film [9], cobalt hexacyanoferrate nanoparticles/gold nanoparticles/multiwalled carbon nanotubes [10] and the determination of H_2O_2, ascorbic acid (AA), dopamine (DA) and uric acid (UA) [11]. Therefore, for many applications, it is necessary to fabricate an inexpensive multifunctional biosensor with redox active thin films for analytical applications of oxidation and reduction side. A variety of compounds have been used for the modification of electrode surfaces with different procedures.

Dopamine (DA), AA and uric acid (UA) usually coexist in human biological system, and are important molecules for physiological processes in human metabolism. There are several reports available about the use of modified electrodes for the simultaneous determination of AA, DA and UA [12 - 16]. It is known that at a bare electrode, the oxidation of AA, DA and UA takes place nearly at the same potential, which results in overlapping voltammetric responses making their discrimination highly difficult [17 - 18].

The selective and sensitive detection of hydrogen peroxide (H_2O_2) has been an important topic of research for decades due to its wide use in many fields, which includes food production [19 - 21], clinical applications [22], oxidation of organic compounds [23 - 25] and fuel cells [26 - 30]. In addition, H_2O_2 is the product of reactions catalyzed by a large number of oxidases. Therefore, determination of H_2O_2 concentration is practically important in the field of biosensor development in order to correlate its concentration to the concentration of target molecules [31 - 35].

In the present work, a novel and stable graphene-AT film modified electrode was prepared by the electro-polymerization of 2-Amino-thiazol (AT) on GCE and dropped graphene on AT/GCE as a graphene-AT/GCE multifunctional biosensor. The interference of AA with DA and UA catalysis was studied at the graphene-AT film modified electrode. Differential pulse voltammetry and amperometric techniques were used to study the oxidation of DA, UA and the reduction of H_2O_2.

2. EXPERIMENTAL

2.1. Materials

2-Amino-thiazol (AT) was purchased from Sigma-Aldrich (USA). Graphene (average particle size = 18 nm) was purchased from Graphene-Supermarket (USA). Double distilled deionized (DDDI) water was used to prepare all solutions. The AT film was prepared by electrochemical polymerization, using 0.1 M H_2SO_4 as supporting electrolyte and the graphene-AT modified electrode tests was prepared using 0.1 M phosphate buffer solution (PBS) as supporting electrolyte (pH 7.0). Pure nitrogen was passed through all the experimental solutions. All the chemicals used were of analytical grade.

2.2. Apparatus

All electrochemical experiments were performed using a CHI 410a potentiostat (CH Instruments, USA). The Bioanalytical Systems (BAS) glassy carbon electrode (GCE; diameter 0.3 cm, exposed geometric surface area 0.07 cm^2; Bioanalytical Systems, Inc., USA) was used. A conventional three-electrode system was used; it comprised a Ag/AgCl (saturated KCl) reference electrode, AT/GCE, graphene/GCE and graphene-AT/GCE modified electrodes, and a bare GCE electrode, as working electrodes, and platinum wire as counter electrode. Electrochemical impedance studies (EIS) were performed using a ZAHNER impedance analyzer (Germany). The atomic force microscope (AFM) images were recorded using a multimode scanning probe microscope (Being Nano-Instruments CSPM-4000, China). Field emission scanning electron microscope (FE-SEM) images were recorded using a HITACHI S-4700 (Japan).

2.3. Preparation of Sample and Hybrid Film Modified Electrode

Prior to the electrochemical deposition process, the GCE was well polished with aqueous slurries of alumina powder (0.05 μm), using a BAS polishing kit, then rinsed and ultrasonicated in DDDI water. To have functional carboxylic group, the acidic treatment of graphene is necessary and has following procedure:

Step 1: Baking graphene to carbonate impurity in the oven at 350 °C for 1 h.

Step 2: Baking graphene in hydrochloric acid (12M) to be dried out, keeping graphene in DDDI water with ultrasonic dispersion for 4 h after.

Step 3: Repeatedly filtering graphene by filter (porosity = 200 nm) in the ultrasonic and DDDI water by 0.1 M PBS (pH 7).

Step 4: Drying the neutralized graphene in the oven at 100 °C for 1h.

Step 5: Keeping graphene in the acidic solution containing sulfuric acid (18M) and nitric acid (18M) (v/v% = 3:1) by ultrasonic dispersion for 6 h.

Step 6: Repeatedly filtering graphene by filter (porosity = 200 nm) in the ultrasonic and DDDI water till neutral condition (pH 7).

Step 7: The neutralized graphene is dried out in the oven at 60 ◦C for 1 h.

Step 8: Finally, the carboxylic is kept in DDDI water to be added on electrode surface.

The inset of Fig. 1A shows the electrochemical polymerization of AT film at GCE in 0.1 M H_2SO_4 solution containing 1 mM AT between -1.5 and +2.0 V, at the scan rate of 0.1 V/s for eight cycles. The AT/GCE was washed with deionized water and dried for 5 min. After polymerization, the carboxylic graphene was added on AT/GCE and dry out to form the graphene-AT/GCE. The graphene-AT/GCE was treated with 0.1 M PBS (pH 7.0) solution by repeated cycling in the potential range –0.2 to +1.0 V, at the scan rate of 0.1 V/s, until a stable cyclic voltammogram (CV) was obtained.

3. RESULT AND DISCUSSION

3.1. Electrochemical properties of graphene-AT film modified GCE

Fig. 1A shows the comparison of cyclic voltammogram of (a) graphene-AT/GCE, (b) graphene/GCE, (c) AT/GCE, and (a') bare GCE in 0.1M PBS (pH 7), respectively. However, (a) graphene-AT film shows interesting redox couples type which is different from those of unique (b) graphene and (c) AT films.

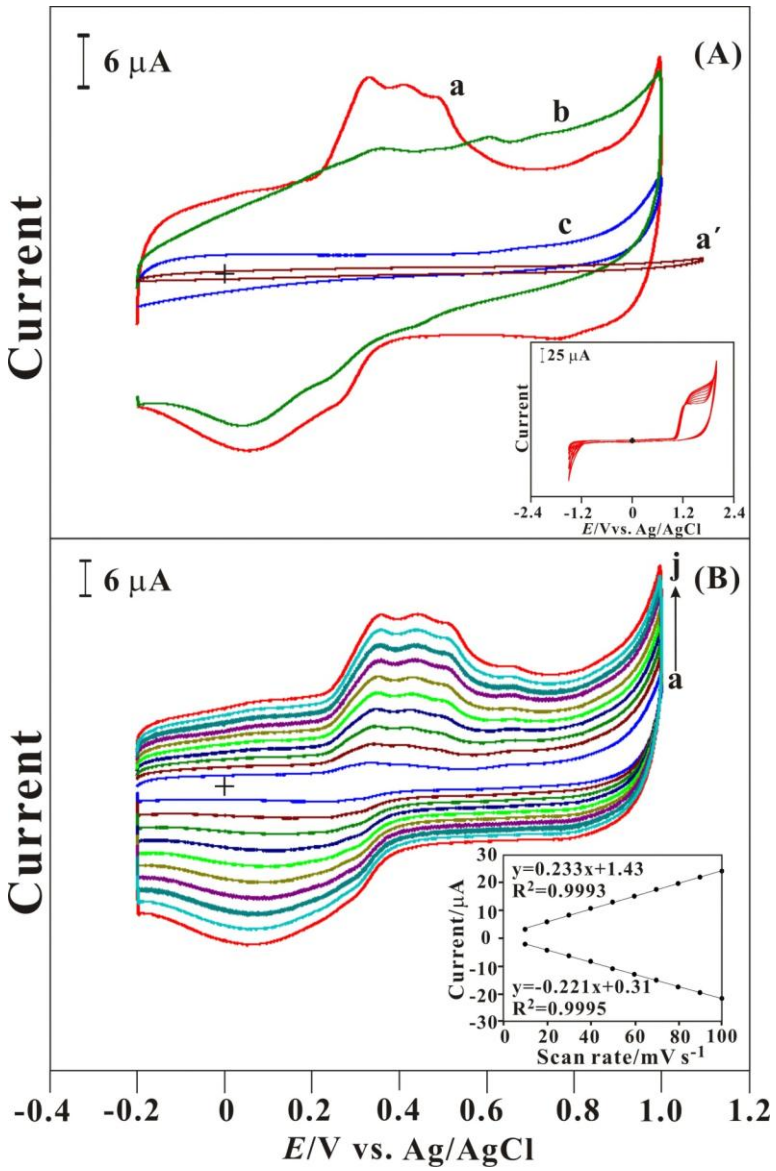

Figure 1 (A) CVs of (a) graphene-AT/GCE, (b) graphene/GCE, (c) AT/GCE and (a') bare GCE in 0.1 M PBS (pH 7.0). Inset: CVs of the GCE by consecutive sweeps in 0.1 M H_2SO_4 solution containing 1 mM AT between -1.5 and +2.0 V. Scan rate = 0.1 V/s. **(B)** Results of different scan rate studies of a graphene-AT/GCE in 0.1 M PBS (pH 7.0). Scan rate in the range of a-j: 0.1-1 V/s. Insets: plot of anodic and cathodic peak current vs. scan rate.

The oxidation and reduction peaks of graphene-AT/GCE are separated as ＋331 and ＋77 mV. When comparing the magnitude of current in 0.1 M PBS (pH 7.0), the current was observed for (a) graphene-AT/GCE was higher than (b) graphene/GCE, (c) AT/GCE and (a') bare GCE. In the same buffer solution, there are no obvious response at curve (b) graphene/GCE, (c) AT/GCE and (a') bare GCE. All the above results indicate that the graphene-AT film modified GCE shows a stable and higher current in 0.1 M pH 7.0 PBS.

The graphene-AT film modified GCE is employed for different scan rate studies in 0.1 M PBS (pH 7.0). Fig. 1B exhibits the different scan rate studies of graphene-AT film modified GCE in the range of (a) 10, (b) 20, (c) 30, (d) 40, (e) 50, (f) 60, (g) 70, (h) 80, (i) 90, (j) 100 mV/s. As expected, the cyclic voltammograms of graphene-AT modified GCE exhibited anodic peaks at +0.34 V, +0.46 V, +0.51, +0.66 V and cathodic peak at +0.09 V vs. $Ag/AgCl/KCl_{sat}$. The inset of Fig. 1B shows the plot of graphene-AT film signal of anodic and cathodic peak current vs. the scan rate. The corresponding linear regression equations were found as I_{pa} (μA) = 0.233v (V/s) ＋ 1.43, R^2 = 0.9993 and I_{pc} (μA) = – 0.221v (V/s) ＋ 0.31, R^2 = 0.9995. This observation indicates that the electron transfer process involves a surface confined species and the charge transfer is fast in the coating [35].

3.2 pH effect and EIS analysis

Fig. 2A shows cyclic voltammograms of graphene-AT film modified electrode of different pH values: (a) pH 1, (b) pH 3, (c) pH 5, (d) pH 7, (e) pH 9, (f) pH 11 and (g) pH 13. The $E^{0'}$ of the redox couple (E_{pa} + E_{pc})/2 was found to shift more negative potential direction and peak currents decreases with increasing pH value. The inset of Fig. 2A shows the plot of $E^{0'}$ vs. the pH value and has a slope of −67 mV per pH for graphene-AT film. The $E^{0'}$ is close to the anticipated Nernstian value of −59 mV/pH for electrochemical processes involving the same numbers of proton and electron transfer.

Next the electrochemical activity of the graphene-AT/GCE has been examined using EIS technique. Here the complex impedance can be presented as a sum of the real, Z' (Ω), and imaginary Z'' (Ω), components that originate mainly from the resistance and capacitance of the cell. From the shape of an impedance spectrum, the electron-transfer kinetics and diffusion characteristics can be extracted.

The respective semicircle parameters correspond to the electron transfer resistance (R_{et}) and the double layer capacity (C_{dl}) nature of the modified electrode. As shown in Fig. 2B, curve (a) indicates the Nyquist plot of graphene-AT/GCE, (b) graphene/GCE, (c) AT/GCE and (a') bare GCE in the presence of 5 mM $K_3[Fe(CN)_6]/K_4[Fe(CN)_6]$ in PBS (pH 7.0).

The graphene/GCE shows a small depressed semi circle arc with an interfacial resistance due to the electrostatic repulsion between the charged surface and probe molecule $Fe(CN)_6^{3-/4-}$. This depressed semi circle arc (R_{et} = 0.38 (Z'/KΩ)) clearly indicates the lower electron transfer resistance behavior comparing with the graphene-AT/GCE (R_{et} = 0.42 (Z'/KΩ)), the AT/GCE (R_{et} = 0.65 (Z'/KΩ)) and bare GCE (R_{et} = 0.73 (Z'/KΩ)). These results clearly illustrate the electrochemical activities of the graphene-AT, graphene, AT films modified GCE and bare GCE, respectively.

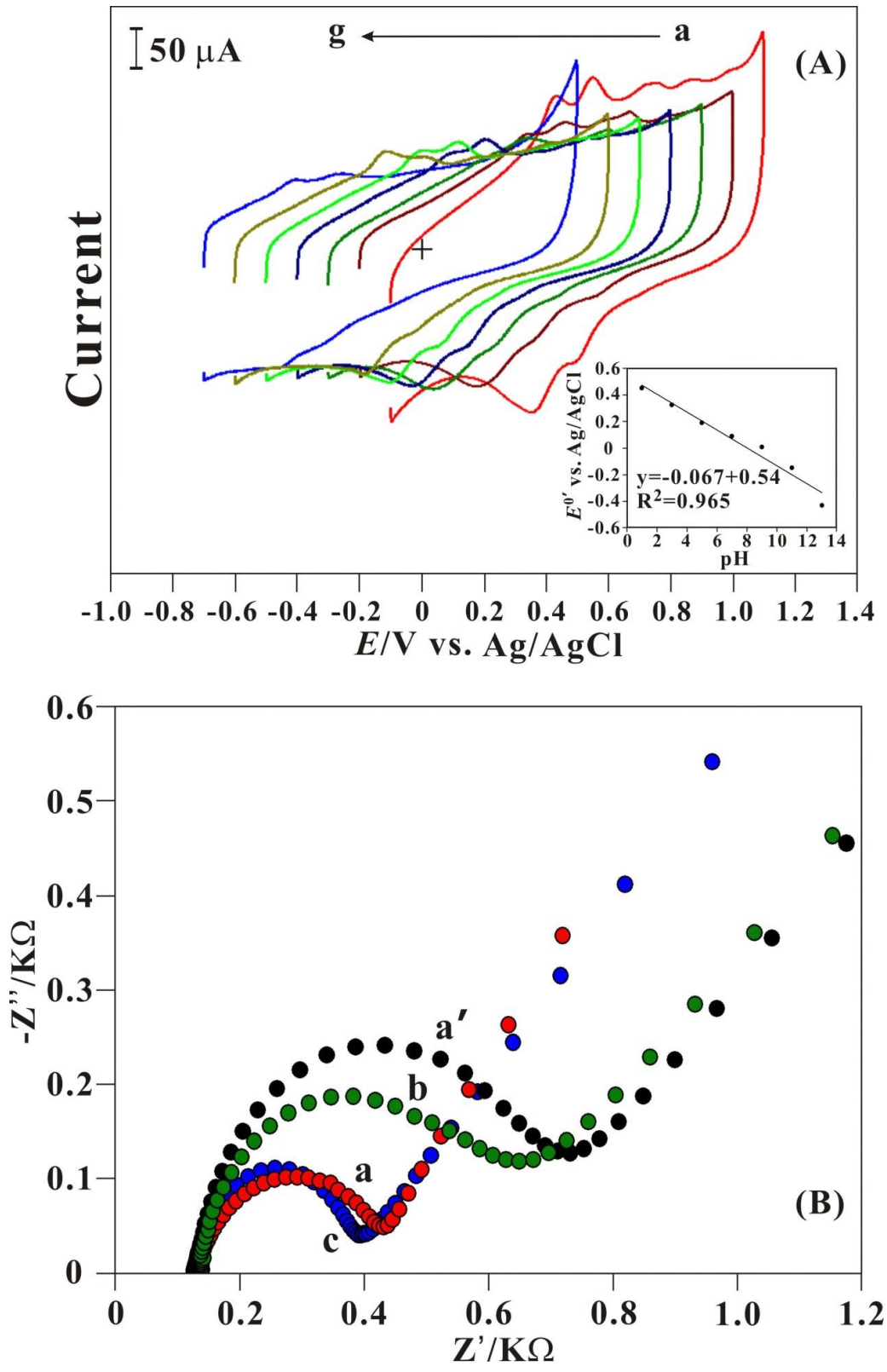

Figure 2. (A) Cyclic voltammograms of graphene-AT/GCE tested with various pH conditions including pH= (a) 1, (b) 3, (c) 5, (d) 7, (e) 9, (f) 11 and (g) 13, scan rate = 0.1 V s^{-1}. Inset: plot of formal potential of graphene-AT/GCE vs. pH values. **(B)** Electrochemical impedance spectra of (a) graphene-AT/GCE, (b) graphene/GCE, (c) AT/GCE, and (a') bare GCE tested in 0.1 M PBS solution (pH 7) containing 5×10^{-3} M $K_3[Fe(CN)_6]/K_4[Fe(CN)_6]$.

3.3 AFM and SEM Analysis of graphene-AT Film

The surface morphology of electro polymeration AT, graphene and graphene-AT films has been examined using AFM and SEM.

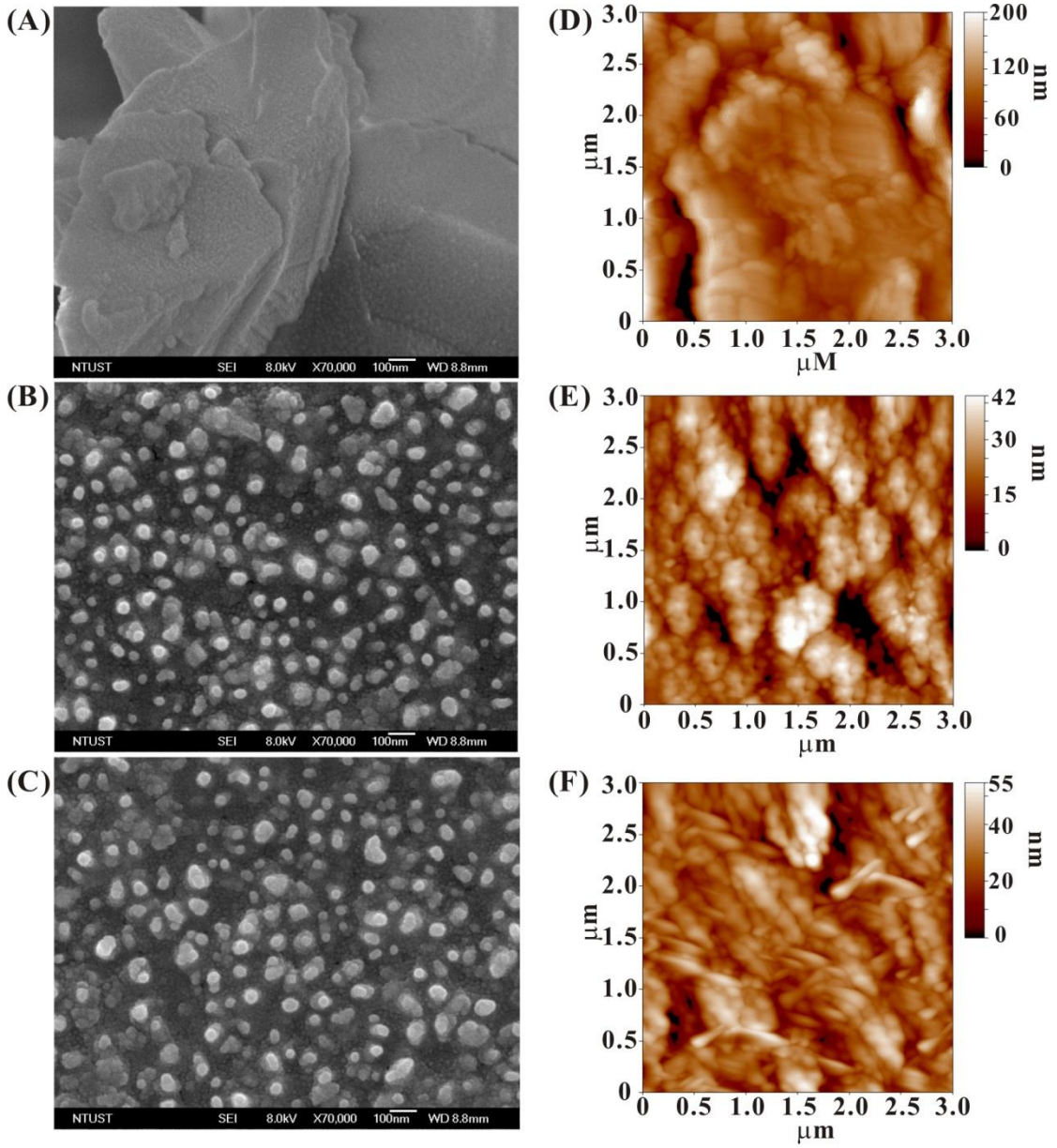

Figure 3. SEM image of a **(A)** graphene film on a GCE, **(B)** AT film on a GCE, **(C)** graphene-AT film on a GCE and Tapping mode AFM image (2D) of **(D)** graphene film on a GCE, **(E)** AT film on a GCE, **(F)** graphene-AT film on a GCE.

Here the studies clearly give the information about the surface morphology of grpahene-AT film coated on the GCE surface. The AFM parameters have been evaluated for 3000×3000 nm surface area by tapping mode. As shown in Fig. 3, the surface morphology of graphene/GCE (A & D), AT/GCE (B & E), and graphene-AT/GCE (C & F) was examined with by SEM and AFM, respectively.

By the AFM images (shown in Fig. 3D–F), the significant average diameter of graphene film, AT film, and graphene-AT film was found 42.6 nm, 36.6 nm, and 43.8 nm, respectively. From SEM images, it is difficult to distinguish the surface morphology of AT/GCE and graphene-AT/GCE. These films modified electrodes have unique features and can be recognized by different surface morphology. By comparison of roughness of these films, graphene (21.3 nm) is obviously bigger than that of AT (7.12 nm) and graphene-AT (7.56 nm). Finally, the above results clearly illustrate the surface nature of graphene, AT and graphene-AT film on the GCE surface.

3.4 Electrocatalytic Properties of graphene-AT Film

3.4.1 Electrocatalytic reduction of hydrogen peroxide at various modified electrode

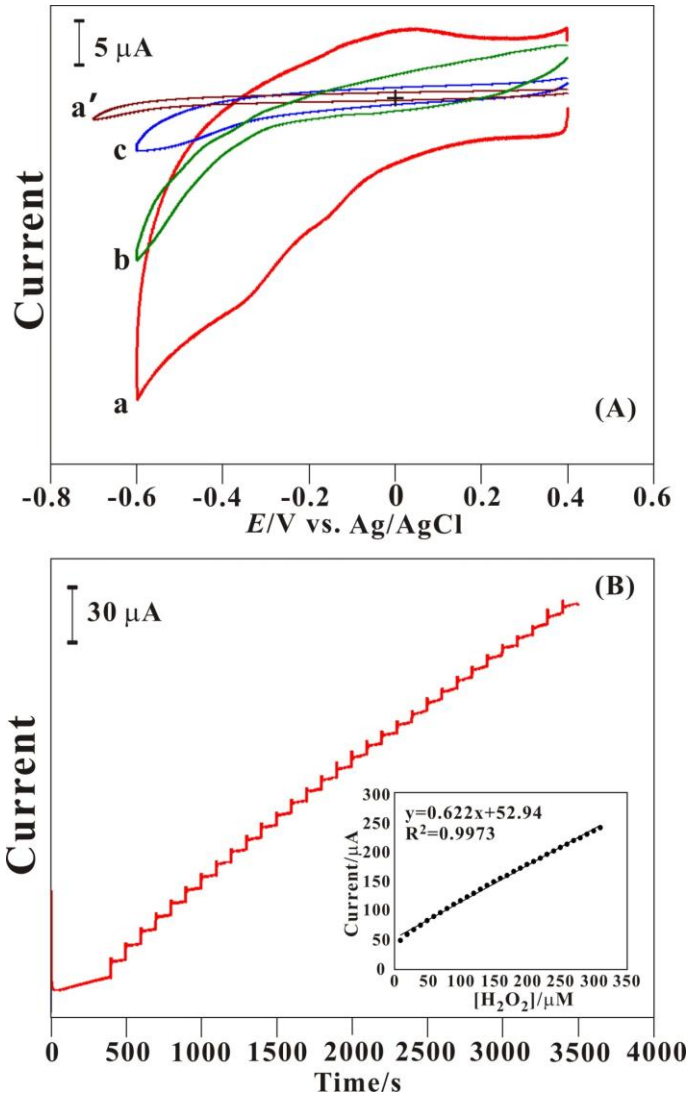

Figure 4. (A) CVs of (a) graphene-AT/GCE, (b) graphene/GCE, (c) AT/GCE and (a') bare GCE in 0.1 M PBS (pH 7.0) containing 10^{-4} M H_2O_2. **(B)** Amperometric responses of H_2O_2 (each 10 μM) tested by graphene-AT/GCE in 0.1 M PBS (pH 7), rotating speed = 1000 rpm, $E_{app.}$ = –0.6 V. Insets: the corresponding calibration plot with the concentration of H_2O_2 between 1×10^{-5} to 3.1×10^{-4} M.

The electrocatalytic reduction of hydrogen peroxide (H_2O_2) is studied and compared with different film modified electrodes in the deoxygenating PBS solution by voltammetry. Fig. 4A shows the cyclic voltammograms of (a) graphene-AT/GCE, (b) graphene/GCE, (c) AT/GCE, and (a') bare GCE examined in 0.1 M PBS (pH 7) solution containing 10^{-4} M H_2O_2, respectively. The proposed composite, (a) graphene-AT/GCE, shows high electrocatalytic reduction current for H_2O_2 comparing to other electrodes. By comparison, the graphene-AT film shows the unique electrocatalytic ability of lower over-potential and higher electrocatalytic current better than that of graphene/GCE, AT/GCE and bare GCE. It represents graphene-AT film has potential to develop a H_2O_2 sensor.

The graphene-AT/GCE is applied in 0.1 M PBS solution (pH 7) with the sequential additions of H_2O_2 by amperometry. Fig. 4B shows the amperometric responses of sequential additions of standard H_2O_2 (each 10 μM) and tested by nano-Au-PEDOT/GCE in 0.1 M PBS (pH 7), respectively, rotating speed = 1000 rpm, $E_{app.}$ = –0.6 V. It could be found linearly dependence between amperometric current and H_2O_2 concentration (shown in the inset of Fig. 4B) during 400－3500 s. For the H_2O_2 detection, the sensitivity of graphene-AT/GCE was 1.73 mA mM^{-1} cm^{-2} and the linear concentration range of H_2O_2 was from 1×10^{-5} to 3.1×10^{-4} M with a correlation coefficient of 0.9973. The detection limit was 1×10^{-6} M with a 'signal-to-noise ratio' of 3. Hence, graphene-AT/GCE for the detection of H_2O_2 also has a higher sensitivity.

3.4.2 Electrocatalytic oxidation of DA and UA at various modified electrode

The electrocatalytic oxidation of AA, DA[36], and UA mixture is studied by cyclic voltammetry and compared with different film modified electrodes in the deoxygenating PBS solution. Fig. 5A shows the electrocatalytic oxidation cyclic voltammograms of AA, DA, and UA mixture containing 1×10^{-5} M AA, 1×10^{-5} M DA, and 5×10^{-5} M UA by (a) graphene-AT/GCE, (b) graphene/GCE, (c) AT/GCE and (a') bare GCE electrodes, respectively. In the AA, DA, and UA mixture in pH 7.0 PBS, there are only two oxidation peaks of DA and UA at graphene-AT/GCE. Compare with graphene/GCE (curve (b)), it also shows two oxidation peaks of DA and UA but the current response is relatively lower than graphene-AT/GCE. Similarly, (c) AT/GCE and (a') bare GCE electrode which always show only one electrocatalytic peak of about 0.23 V and 0.41 V for AA, DA, and UA mixture during scanning potential range from −0.2 to 1.0 V. Significant electrocatalytic potential and current were observed by these film modified electrodes. Particularly, graphene-AT/GCE only has oxidation current response for DA and UA, but no oxidation current response for AA. It means that graphene-AT/GCE has its specific electrocatalytic property with higher electrocatalytic oxidation current for DA and UA in the presence of AA, DA and UA mixture.

As shown in Fig. 5B, the individual electrocatalytic oxidation of DA and UA were investigated using differential pulse voltammetry (DPV). The graphene-AT/GCE reduces the anodic over potentials and exhibits well-defined anodic peaks for DA and UA oxidation (0.206 and 0.348 V) and the peak separations between DA and UA (0.142 V) is sufficient enough to exhibit them as a well-defined three separate peaks. Further the simultaneous determination of DA and UA concentrations was in the linear

range of 0–2.5×10^{-5} and 0–1.25×10^{-4} M, respectively. Here all the oxidation peak currents increase linearly with respect to their increasing concentrations.

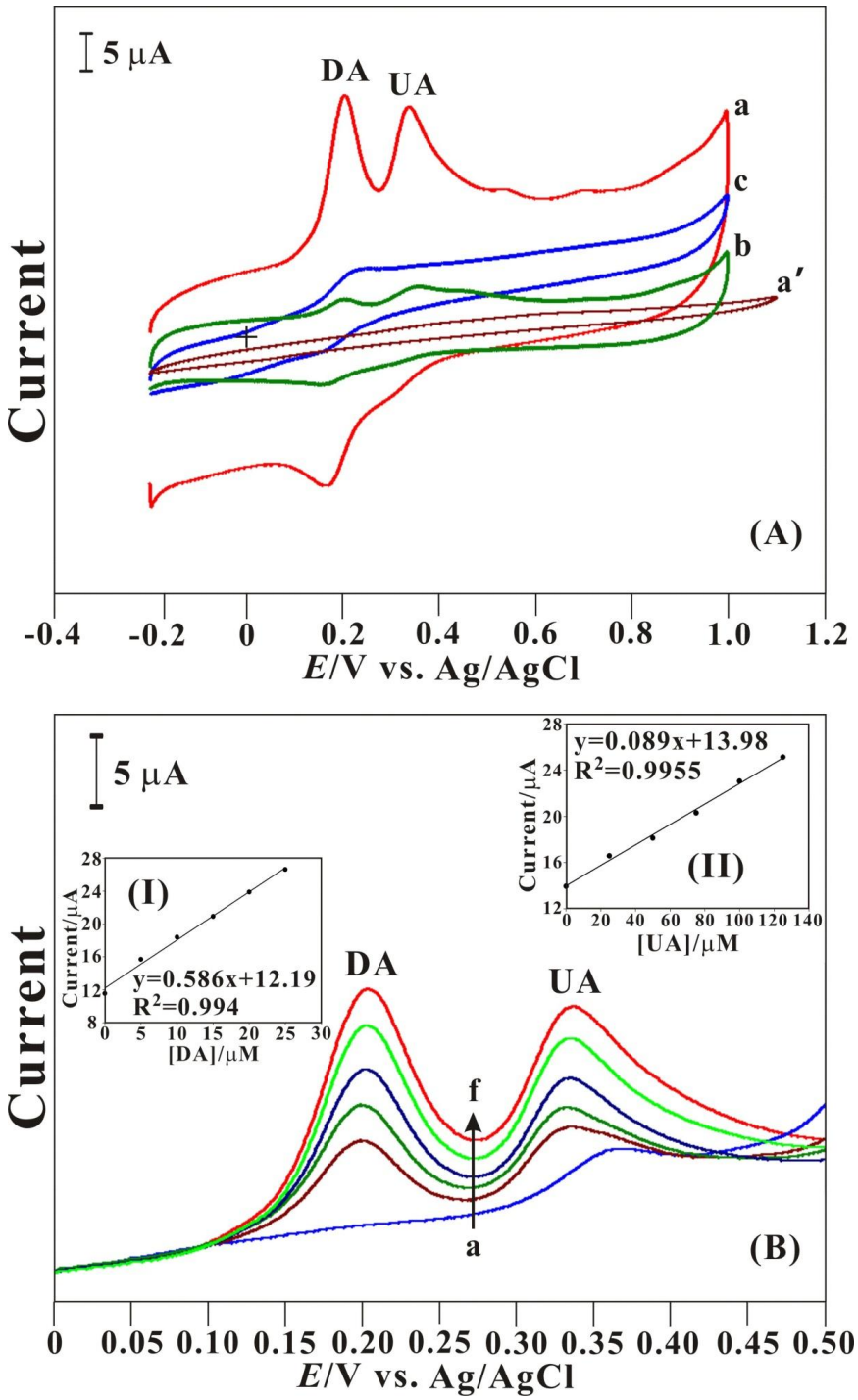

Figure 5. (A) CVs of (a) graphene-AT/GCE, (b) graphene/GCE, (c) AT/GCE and (a') bare GCE in 0.1 M PBS (pH 7.0) containing 1×10^{-5} M AA, 1×10^{-5} M DA, and 5×10^{-5} M UA. **(B)** Differential pulse voltammetry of graphene-AT film for the detection of DA and UA in 0.1 M PBS (pH 7.0). Inset: calibration plot of oxidation current vs. concentration of (I) DA were in the range of (a – f): 0, 5, 10, 15, 20 and 25 μM. (II) UA concentrations were in the range of (a – f): 0, 25, 50, 75, 100 and 125 μM.

From the calibration plots the linear regression equations for DA and UA were expressed as I_{pa} (μA) = 0.5856*C* (10^{-6} M)+12.193, R^2 = 0.994 and I_{pa} (μA) = 0.0885*C* (10^{-6} M)+13.983, R^2 = 0.9955, as show in the inset (I) and (II) of Fig. 5B. The relative standard deviation (% RSD) for all the determination on the graphene-AT/GCE was less than 2.0% which shows the efficiency and linear nature of graphene-AT/GCE. Finally, from these DPV results, it can be concluded that the graphene-AT/GCE is a suitable mediator for the simultaneous determination of DA and UA with AA interference.

3.4.3 Selective detection of dopamine and uric acid

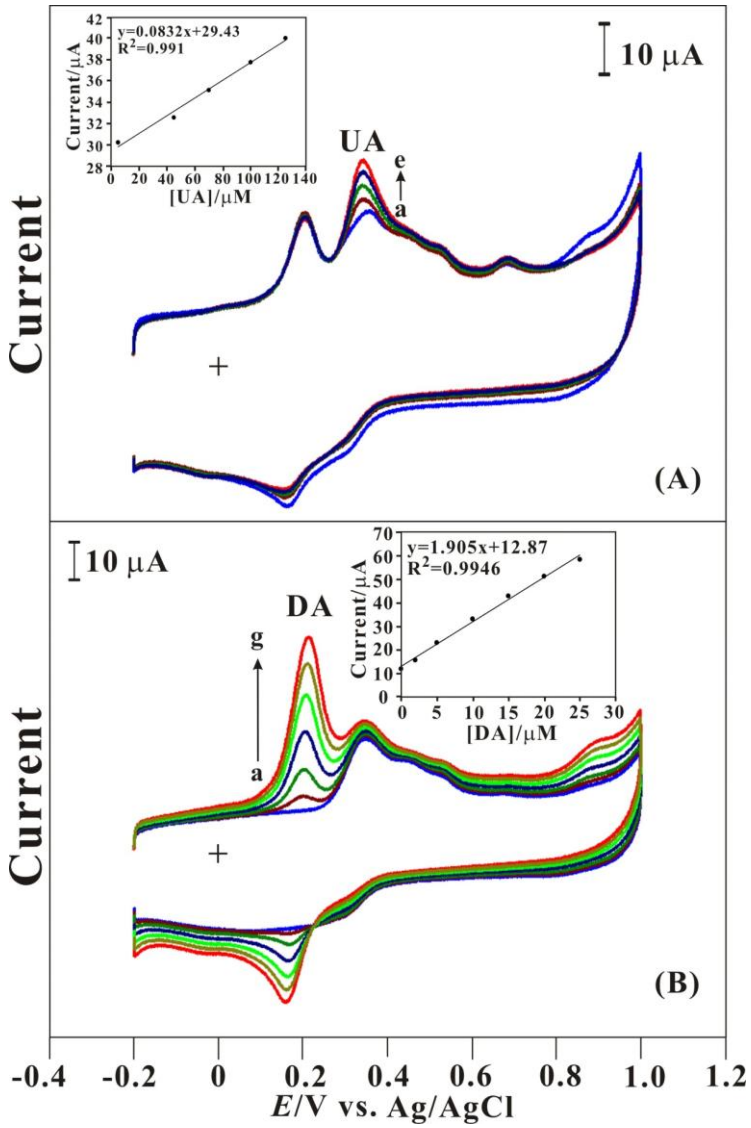

Figure 6. (A) CVs of graphene-AT/GCE in 0.1 M PBS (pH 7.0) with the mixture of 1×10^{-5} M AA, DA and various concentrations of UA. UA concentration: (a) 5, (b) 45, (c) 70, (d) 100 and (e) 125 μM. Inset: calibration plot of oxidation current vs. concentration of UA. **(B)** CVs of graphene-AT/GCE in 0.1 M PBS (pH 7.0) with the mixture of 1×10^{-5} M AA, 5×10^{-5} M UA and various concentrations of DA. DA concentration: (a) 0, (b) 2, (c) 5, (d) 10, (e) 15, (f) 20 and (g) 25 μM. Inset: calibration plot of oxidation current vs. concentration of DA.

Fig. 6A exhibits the CVs of UA in the presence of 1×10^{-5} M AA and DA in PBS (pH 7.0) at the graphene-AT/GC electrode. The voltammetric peak corresponding to the oxidation of UA was found increased linearly in consonance with the increase of the bulk concentration of UA whereas no current response for AA and slightly decrease the current response of DA. The inset of Fig. 6A shows that the linearly calibration plot for UA with a slope of 1.19 mA mM^{-1} cm^{-2}. By the same way, Fig. 6B shows the CVs response of the graphene-AT/GC electrode in the presence of 1×10^{-5} M AA and 5×10^{-5} M UA in PBS (pH 7.0) and continues addition of DA. The inset of Fig. 6B shows that the calibration plot for DA was linear with a slope of 27.2 mA mM^{-1} cm^{-2}. The voltammetric peak corresponding to the oxidation of DA was found increase linearly with continues addition of DA, whereas no current response was observed for AA but a slight increase in the peak current of UA. The above results confirmed that the responses of DA and UA at the graphene-AT/GC electrode are independent even AA is present.

3.5. Stability and Reproducibility of graphene-AT/GCE multifunctional biosensor

The reproducibility of the biosensor was examined by measuring H_2O_2, DA and UA, and the relative standard deviation was less than 2.0 (n = 5). It was indicated that the multifunctional biosensor possess good reproducibility. In addition, the catalytic current responses for H_2O_2, DA and UA at graphene-AT/GCE were tested in pH 7.0 PBS containing H_2O_2, DA and UA before and after continuously stirring the buffer solution for 30 min. The electrode current had no significant change before and after stirring the solution; this test indicate that reproducible results can be obtained at graphene-AT/GCE. The stability of graphene-AT/GCE was then investigated by storing it at room temperature in the presence and absence of PBS (pH 7.0). It was stable for one month but thereafter there was a gradual decrease (10%) in the current values. When the graphene-AT/GCE stored for one week in pure PBS (pH 7.0), the current response of H_2O_2, DA and UA were decreased less than 9% of the initial current. These results suggest that the graphene-AT/GCE has high stability and good reproducibility.

4. CONCLUSIONS

Here we report an electrochemical method to form a stable graphene-AT film modified on GCE. The electrochemical behaviors and surface analysis of graphene-AT, graphene and AT films have been studied by voltammetry, EIS, SEM and AFM. The formal potential of graphene-AT film was found -67 mV/pH and similar to the Nernstian equation involved the same numbers of proton and electron transfer. Furthermore, graphene-AT/GCE can be a multifunctional biosensor and provides good sensitivity, selectivity and stability for H_2O_2, DA and UA with AA interference.

ACKNOWLEDGMENT
This work was supported by the National Science Council of Taiwan.

References

1. R.W. Murray, in Bard, A.J. (Ed.), Electroanalytical Chemistry, Marcel Dekker, New York, 1983.
2. A.E. Gorshteyn, A. Robbat, Jr., *Ind. Eng. Chem. Res.* 39 (2000) 2006–2009.
3. L.J.J. Janssen, L. Koene, *Chem. Eng. J.* 85 (2002) 137–146.
4. K.S. Yun, J. Gil, J. Kim, H.J. Kim, K. Kim, D. Park, M. Kim, H. Shin, K. Lee, J. Kwak, E. Yoon, *Sens. Actuators* B 102 (2004) 27–34.
5. J. Wang, *Trends Anal. Chem*. 21 (2002) 226–232.
6. Y. Torisawa, N. Ohara, K. Nagamine, S. Kasai, T. Yasukawa, H. Shiku, T. Matsue, *Anal. Chem.* 78 (2006) 7625–7631.
7. M. Albareda-Sirvent, A. Merkoci, S. Alegret, *Sens. Actuators* B 69 (2000) 153–163.
8. M. Yang, J. Jiang, Y. Lu, Y. He, G. Shen, R. Yu, *Biomaterials* 28 (2007) 3408–3417.
9. Y. Wang, W. Wei, X. Liu, X. Zeng, *Materials Science and Engineering* C 29 (2009) 50–54.
10. S. Wang, L. Lu, M. Yang, Y. Lei, G. Shen, R. Yu, *Analytica Chimica Acta* 651 (2009) 220–226.
11. K.C. Lin, T.H. Tsai, S.M. Chen, *Biosensors and Bioelectronics* 26 (2010) 608–614.
12. S. Thiagarajan, T.H. Tsai, S.M. Chen, *Biosens. Bioelectron*. 24 (2009) 2712–2715.
13. H.R. Zare, N. Nasirizadeh, M. Mazloum-Ardakani, *J. Electroanal. Chem*. 577 (2005) 25–33.
14. A.Balamurugan, S.M. Chen, *Anal. Chim. Acta* 596 (2007) 92–98.
15. J. Mathiyarasu, S. Senthilkumar, K.L.N. Phani, V. Yegnaraman, *Mater. Letters* 62 (2008) 571–573.
16. S. Harish, J. Mathiyarasu, K.L.N. Phani, V. Yegnaraman, *J. Appl. Electrochem.* 38 (2008) 1583–1588.
17. T.H. Tsai, T.W. Chen, S.M. Chen, *Electroanalysis* 22 (2010) 1655–1662.
18. H. Elzanowska, E. Abu-Irhayem, B. Skrzynecka, V. I. Birss, *Electroanalysis* 16 (2004) 478–490.
19. F.M. Jin, A. Kishita, T. Moriya, H. Enomoto, *J. Supercrit. Fluid* 19 (2001) 251–262.
20. A.Salimi, R. Hallaj, S. Soltanian, H. Mamkhezri, *Anal. Chim. Acta* 594 (2007) 24–31.
21. E. Swift, H. Heymann, A. Wilder, A. St-Georges, M. Nunes, *J. Dent. Res.* 81 (2002) 253–258.
22. Y.P. Huang, J. Li, W.H. Ma, M.M. Cheng, J.C. Zhao, J.C. Yu, *J. Phys. Chem*. B 108 (2004) 7263–7270.
23. S.R. Sarathy, M. Mohseni, *Environ. Sci. Technol*. 41 (2007) 8315–8320.
24. Y. Usui, K. Sato, M. Tanaka, *Angew. Chem. Int. Ed*. 42 (2003) 5623–5625.
25. N.A. Choudhury, R.K. Raman, S. Sampath, A.K. Shukla, *J. Power Sources* 143 (2005) 1–8.
26. E. Kjeang, A.G. Brolo, D.A. Harrington, N. Djilali, D. Sinton, *J. Electrochem. Soc.* 154 (2007) B1220–B1226.
27. G.H. Miley, N. Luo, J. Mather, R. Burton, G. Hawkins, L.F. Gu, E. Byrd, R. Gimlin, P.J. Shrestha, G. Benavides, J. Laystrom, D. Carroll, *J. Power Sources* 165 (2007) 509–516.
28. R.K. Raman, A.K. Shukla, *Fuel Cells* 7 (2007) 225–231.
29. A.Ramanavicius, A. Kausaite, A. Ramanaviciene, *Biosens. Bioelectron*. 20 (2005) 1962–1967.
30. S. Cosnier, S. Szunerits, R.S. Marks, A. Novoa, L. Puech, E. Perez, I. Rico-Lattes, *Electrochem. Commun.* 2 (2000) 851–855.
31. M.D. Gouda, M.A. Kumar, M.S. Thakur, N.G. Karanth, *Biosens. Bioelectron*. 17 (2002) 503–507.
32. J.X. Wang, X.W. Sun, A. Wei, Y. Lei, X.P. Cai, C.M. Li, Z.L. Dong, *Appl. Phys. Lett*. 88 (2006) 233106-1–233106-3.
33. A.Wei, Sun, X.W., Wang, J.X., Lei, Y., Cai, X.P., Li, C.M., Dong, Z.L., Huang, W., 2006. *Appl. Phys. Lett.*, 89, 123902-1–123902-3.
34. Y.J. Zou, C.L. Xiang, L.X. Sun, F. Xu, *Biosens. Bioelectron*. 23 (2008) 1010–1016.
35. E. Laviron, L. Roullier, C. Degrand, *J. Electroanal. Chem*. 112 (1980) 11–23.
36. S.-M. Chen, K.-T. Peng, *J. Electroanal. Chem.*, 547,(2003), 179-189.